Separation Science and Technology
Publication details, including instructions for authors and subscription information:
http://www.informaworld.com/smpp/title~content=t713708471

A Study of the Mass Transfer of CO_2 through Different Membrane Materials in the Membrane Gas Absorption Process

Julianna Franco[a]; David deMontigny[b]; Sandra Kentish[a]; Jilska Perera[a]; Geoff Stevens[a]
[a] Department of Chemical and Biomolecular Engineering, The Cooperative Research Centre for Greenhouse Gas Technologies, The University of Melbourne, Victoria, Australia [b] Faculty of Engineering, The International Test Centre for Carbon Dioxide Capture, University of Regina, Saskatchewan, Canada

To cite this Article Franco, Julianna , deMontigny, David , Kentish, Sandra , Perera, Jilska and Stevens, Geoff(2008) 'A Study of the Mass Transfer of CO_2 through Different Membrane Materials in the Membrane Gas Absorption Process', Separation Science and Technology, 43: 2, 225 — 244
To link to this Article: DOI: 10.1080/01496390701791554
URL: http://dx.doi.org/10.1080/01496390701791554

Separation Science and Technology, 43: 225–244, 2008

ISSN 0149-6395 print/1520-5754 online
DOI: 10.1080/01496390701791554

A Study of the Mass Transfer of CO_2 through Different Membrane Materials in the Membrane Gas Absorption Process

Julianna Franco,[1] David deMontigny,[2] Sandra Kentish,[1] Jilska Perera,[1] and Geoff Stevens[1]

[1]The Cooperative Research Centre for Greenhouse Gas Technologies, Department of Chemical and Biomolecular Engineering, The University of Melbourne, Victoria, Australia
[2]The International Test Centre for Carbon Dioxide Capture, Faculty of Engineering, University of Regina, Saskatchewan, Canada

Abstract: The mass transfer of carbon dioxide through hydrophobic membrane materials into aqueous solutions of monoethanolamine has been studied. Microporous polypropylene, polytetrafluoroethylene and polyvinylidene fluoride hollow fiber membranes were compared. Membranes were characterized before and after use and wetting studies showed that the mass transfer resistance increased by 15% for polypropylene after 45 hours. Wetting may be due to membrane degradation as a result of contact with the solvent. This study highlights the need to choose membrane-solvent systems that utilize a low cost membrane that remains unwetted by the solvent over long periods and when subjected to reasonable solvent-side pressures.

Keywords: Carbon dioxide, mass transfer, absorption, polypropylene, hydrophobicity, monoethanolamine

INTRODUCTION

Power plants are the single largest generators of anthropogenic greenhouse gases (and account for approximately 80% of global energy use) and

Received 1 May 2007, Accepted 17 October 2007
Address correspondence to Geoff Stevens, The Cooperative Research Centre for Greenhouse Gas Technologies, Department of Chemical and Biomolecular Engineering, The University of Melbourne, Victoria 3010, Australia. E-mail: gstevens@unimelb.edu.au

according to the Intergovernmental Panel on Climate Change (IPCC), energy use will continue to be dominated by fossil fuels until at least the middle of the next century (1). Each coal fired power plant emits around 200 mega tonnes of CO_2 equivalents annually. It is envisioned that it will be technically feasible to construct capture plants at many of these sites in order to separate CO_2 for storage underground. Technology exists to separate CO_2 from flue gases, but it would nearly double the current production cost of electricity (2). Membrane gas absorption (MGA) will potentially reduce these costs.

MGA involves the transfer of CO_2 through a non-selective hollow fiber or flat sheet membrane before it is chemically absorbed into a solvent. The use of solvents and membranes are integrated in order to exploit the benefits of both technologies. Most notably, membrane contactors allow for a reduction in equipment sizes. Depending on the hollow fiber dimensions and allowing for practical considerations such as pressure drop, an interfacial area between 500–1000 m^2/m^3 can be achieved by a membrane contactor which is 4–5 times higher than that of a column (3). The other major advantage is the physical separation of the liquid and gas flow rates and consequently an elimination of foaming, a reduction in liquid channelling and the ability to operate the unit in any orientation.

For packed column CO_2 absorption, monoethanolamine (MEA) or similar amine blends are preferred because they surpass the commercially available alternatives by having a relatively high loading capacity, rapid absorption rate, and low cost for regeneration (4). However, solvent-membrane compatibility becomes an equally important criterion in membrane gas absorption because the polymeric membrane is in direct contact with the solvent and vulnerable to chemical attack. Further, if the pores of the membrane are wetted by the solvent, the membrane can introduce a significant resistance to the CO_2 mass transfer rate. It has been shown that the membrane mass transfer coefficient is appreciably higher for the case of non-wetted pores relative to that of wetted pores (5) due to the four-fold increase in the mass transfer coefficient through gas-filled pores relative to liquid-filled pores. The membrane mass transfer coefficient will also depend on membrane porosity, tortuosity, and thickness.

The degree of hydrophobicity required to ensure gas-filled pores will depend upon a number of parameters. The breakthrough pressure (P_{BP}) can be used to predict this wettability of the membrane under processing conditions. This parameter is defined as the pressure that must be applied to a liquid for it to penetrate through the pores of a membrane. Theoretically, it is given by:

$$P_{BP} = -\frac{4\gamma_{lg}\cos\theta}{d_{max}} \tag{1}$$

where γ_{lg} is the surface tension of the solution, θ is the contact angle of the solution on the membrane and d_{max} is the maximum pore diameter.

Regardless of these issues, the criteria for membrane selection should also include an appropriate membrane pore size (0.01–0.5 μm), high porosity,

minimal thickness, high resilience (durability to solvent exposure, fouling, and mechanical stability), and low cost.

Ideally, a membrane cartridge will be used for a period of years before needing to be replaced due to solvent degradation/wetting and fouling. An economic balance needs to be found to ensure a membrane is chosen that has a low resistance to mass transfer that is sustained for a reasonable amount of time but also has a low enough cost. The cost of purchasing and changing a membrane cartridge and the associated downtime should be considered.

Various researchers have studied the CO_2 mass transfer rate in a range of solvent-membrane systems but in many cases, these figures cannot be compared due to differences in operating conditions. The number of studies that focus on the use of MEA or other amine solvents is even more limited. deMontigny et al. (6) compared the performance of polypropylene (PP) and polytetrafluoroethylene (PTFE) using amine solvents. They found that the performance of PP declined with time while PTFE maintained its superior performance. Nishikawa et al. (7) also found that PTFE maintains its performance by conducting experiments with MEA for over 6,600 hours. There has been some work in the manufacture of polyvinylidene fluoride (PVDF) membranes (8, 9) and their performance has generally been found to be favourable. Yeon et al. (10) compared the performance of PVDF and PTFE using MEA and found PVDF to provide a higher rate of mass transfer because it maintained non-wetted pores while the pores of PTFE became semi-wetted. However, it may be argued that this was not a fair comparison of the membrane materials since the PTFE had a higher average pore size than the PVDF (1 μm compared with 0.03 μm). Matsumoto et al. (11) compared PVDF, PE, and PTFE membrane materials and found that PTFE had the highest membrane resistance presumably due to its large pore size (1 μm). However, the membrane contributed only 8% of the total resistance despite the high concentration (30 wt.%) of MEA used. Novel membrane materials have also been prepared and compared with the commercially available alternatives. Polyethylene (PE) coated with a fluoropolymer has been compared with PP, PE, and PTFE by Nishikawa et al. (7). They found that this treatment improved the properties of the membrane relative to PE but that over time, the performance of the treated membrane still degraded.

In this work we compare the performance of PP, PTFE, and PVDF hollow fiber membranes when used with aqueous MEA and provide information about the underlying solvent-membrane compatibilities.

EXPERIMENTAL SECTION

Absorption Experimental Setup

Industrial grade CO_2 (Praxair, Canada) was mixed with air in the proportion 14:86 by volume to simulate a flue gas stream. Analytical grade MEA (Fisher

Scientific, USA) was diluted with deionized water to 10–30 wt.% and preloaded to 0.27–0.30 mol CO_2/mol MEA by bubbling CO_2 through the solution using a sintered glass sparger before use to simulate use of a regenerated solution. Standard 1 M hydrochloric acid (Fisher Scientific, USA) was used for titrations.

The apparatus used is shown in Fig. 1 and the membrane cartridge specifications are given in Table 1. The fibers for two of these cartridges (PP, PTFE) were sourced from commercial suppliers while the PVDF fibers were manufactured on a laboratory scale using the phase inversion method (8). Gas flow controllers (Aalborg, NY, USA) which were calibrated using a digital bubble flow meter (Humonics Optiflow, USA) were used to regulate the gas flows before they entered a pipe mixer and filter. A magnetic drive gear pump (Cole Parmer, IL, USA) pumped MEA solution through a liquid filter and rotameter before being passed through the membrane contactor. The liquid passed through a liquid trap before entering the outlet tank to create a positive liquid head and prevent gas entrainment. Analog pressure readings were available for the differential pressure across both the gas and liquid phases and also for the liquid inlet and outlet (Ashcroft, CT, USA). Temperature readings were taken at the inlet and outlet points for the fluid flowing through the fiber lumen and three equally spaced points along the membrane contactor for the shell side fluid using J-type thermocouples and a calibrated temperature indicator (Omega Engineering Inc., CT, USA).

The CO_2 gas phase concentration was measured using an infra-red gas analyser (Hamilton, ON, Canada). CO_2 liquid loading and MEA concentration were measured with a Chittick Carbon Dioxide Analyser (VWR International, AB, Canada) according to the procedure outlined by the Association of Official Analytical Chemists (12). A known volume of loaded MEA solution was placed into a volumetric flask and connected to the gastight titration apparatus. The MEA concentration was determined by titrating with 2 M HCl solution using methyl orange indicator. Excess HCl was added to ensure all the CO_2 had

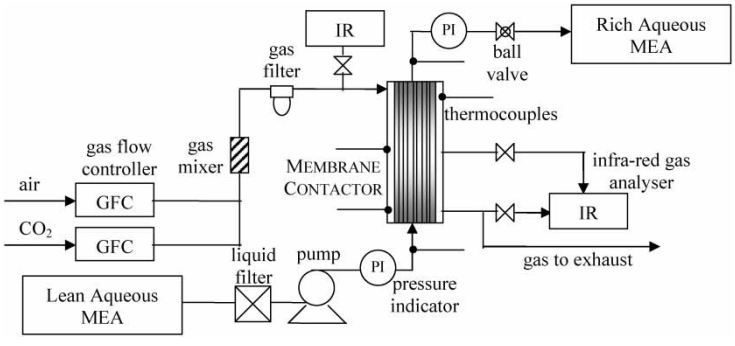

Figure 1. Hollow fiber membrane gas absorption apparatus for liquid flow through the fiber lumen.

Table 1. Properties of membrane modules. PP-polypropylene, PTFE-polytetrafluorotheylene, and PVDF-polyvinylidene fluoride

Polymer type	PP	PTFE	PVDF
Manufacturer	Memtec (Australia)	Sumitomo Electric Fine Polymer (Japan)	Manufactured on laboratory scale at the University of Bath
Price (USD/m)	0.020	14.0	—
Fiber ID/OD (mm)	0.3/0.67	1/2	0.51/0.69
No. of fibers	275, 500	27	264
Contactor length (cm)	12.7	11.0	12.5
Mass transfer area, based on ID/OD (cm^2)	329/735, 598/1337	93/187	527/715
Membrane contactor void fraction (%)	84, 71	86	84
Average pore size (μm)	0.2	$20 \times 2^{a,b}$	0.45^a
Membrane porosity (%)	50	50	10^a

[a]Determined from SEM images.
[b]Pores are non-cylindrical.

been released from the solution. A metering tube filled with standard solution was displaced by both the addition of HCl and freed CO_2. The CO_2 loading of the MEA solution could therefore be back-calculated. The standard solution in the metering tube was made by dissolving NaCl in distilled water. A small amount of $NaHCO_3$ and methyl orange indicator were dissolved in the solution before 1 M HCl was added until the solution turned pink.

For a typical absorption experiment, the gas flow was started first (1 L/min CO_2 and 6.1 L/min air). After consistency in the CO_2 concentration at the contactor inlet and outlet was ascertained using an IR gas analyser, the liquid flow was started (18–85 mL/min). A ball valve was adjusted to increase the outlet liquid pressure to approximately 0.1 bar higher than the gas phase inlet pressure to prevent gas bubbling through the liquid. The liquid flow rate was measured at the outlet using a measuring cylinder. The CO_2 gas phase concentrations at equilibrium at the contactor inlet, outlet and (for shell side gas flow) mid-point were measured and used to calculate the overall mass transfer coefficient. Liquid CO_2 loading was also measured to complete a mass balance for CO_2 absorption across the hollow fiber unit to verify the quality of each experiment. A tolerance of $\pm 5\%$ error for the mass balance was employed.

Membrane Characterization Apparatus

A contact angle goniometer (equipped with FTÅ200 analysis software) was used to measure the contact angle of both distilled water and 20 wt.% MEA solution on flat sheet membranes. Water contact angles were tested on fresh

membranes and membrane that had been exposed to 20 wt.% MEA solution for 2 days. The same instrument was used to determine the interfacial tension of the MEA solutions.

Breakthrough pressure measurements were conducted to find the liquid entry pressure of the membranes by pressuring a solution of 20 wt.% isopropanol (Sigma Aldrich, Australia) which has a surface tension of 34 mN/m on supported porous flat sheet membranes using nitrogen gas. A digital pressure gauge was used to monitor the step-wise increase in gas pressure by 1 kPa/minute. Breakthrough of the solution was visually observed and an average of 10 measurements was conducted per membrane type to allow for variability between membrane sheets.

Several membrane analysis techniques were used before and after absorption experiments. Scanning electron microscopy (SEM) was conducted using a JEOL JSM-5600 SEM (Akishima-Shi, Japan) with a tungsten hairpin filament, power of 10 kV, working distance of approximately 20 mm and magnification ranging from 150–2000×. A spot size or electron beam diameter of 36 ensured an adequate resolution and minimal sample damage. Samples were attached to aluminum stubs using carbon tabs and sputtered coated with a conducting material to prevent the samples from charging. Membranes were also analyzed using X-ray photoelectron spectroscopy (XPS). XPS was performed using an Axis Ultra spectrometer (Kratos Analytical, UK) equipped with a monochromatized X-ray source operating at 150 W.

RESULTS AND DISCUSSION

Absorption Rates

Figure 2 gives a visual representation of the absorption process in a membrane contactor system.

The CO_2 flux (N) through the membrane contactor is given by:

$$N = \frac{(Y_{in} - Y_{out})G}{A} \tag{2}$$

where Y is the mole ratio of CO_2 in the gas phase, G is the inert gas flow rate, and A is the mass transfer area.

The CO_2 flux through each membrane type calculated from this equation is shown in Fig. 3. PTFE gives the highest CO_2 absorption flux followed by PP and then PVDF. The superior performance of PTFE is likely due to its high degree of hydrophobicity and this has been explored further in the next section. It has already been established on a laboratory scale that PTFE maintains its high performance over time when used with MEA (6, 7). but this may not justify its high cost. Given the extremely low price of PP

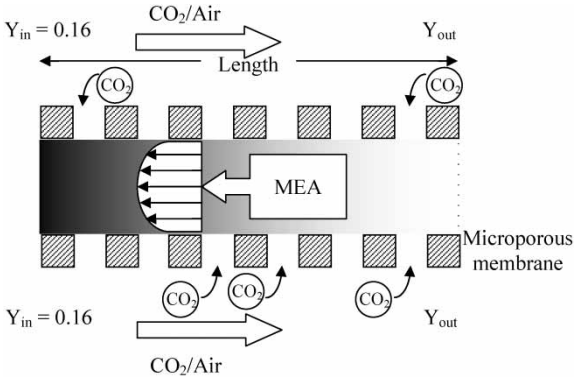

Figure 2. Schematic diagram of CO_2 mass transfer through a singe hollow fiber membrane with liquid flow through lumen.

fibers and their satisfactory absorption performance, this membrane material was chosen for further testing.

The overall mass transfer coefficient (K_G) in the contactor was calculated using a similar method to that used for absorption in a packed column system (13) (see Appendix A).

$$K_G a_v = \frac{G}{P_T(y - y^*)} \frac{dY}{dx} \tag{3}$$

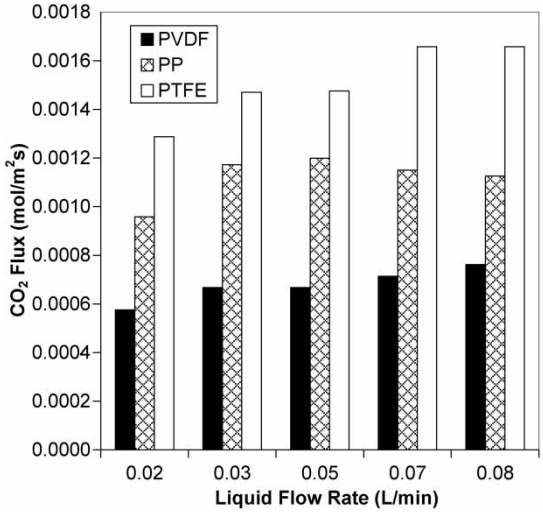

Figure 3. Membrane comparison based on CO_2 flux using 20 wt.% MEA solution. Liquid flow through fiber lumen.

where a_v is the specific surface area, P_T is the total pressure, y is the mole fraction of CO_2 in the gas phase, and x is the contactor length. For chemical absorption, the equilibrium mole fraction of CO_2 in the gas phase (y^*) is assumed to be zero.

This overall gas phase mass transfer coefficient can further be considered in terms of a series of resistances to mass transfer through:

$$\frac{1}{K_G} = \frac{1}{k_g} + \frac{1}{k_m} + \frac{1}{mEk_l} \tag{4}$$

where k_g, k_m, and k_l are the gas, membrane and liquid side mass transfer coefficients respectively, m is the partition coefficient, and E is the enhancement factor due to chemical reaction.

Table 2 uses the overall mass transfer coefficient to show how the performance of PP changes over longer periods of absorption. As the exposure time of the fibers to MEA is increased, the mass transfer rate reduces. Over a period of 165 hours, no lower limit was reached. It must be therefore assumed that the mass transfer rate will continue to decrease for periods of absorption longer than 165 hours.

In addition to this degradation in performance with the time of contact between MEA and PP, a drop in performance is also evident from increasing the MEA concentration in the liquid phase. Figure 4 shows that at MEA concentrations of 10–20 wt.% the mass transfer coefficient increases with MEA concentration as a consequence of an increasing enhancement factor (i.e. an increase in E in Equation (4)). The mass transfer performance also increases as the liquid flow rate increases which can be related to increasing turbulence in the liquid side boundary layer (i.e. an increase in k_l).

A dramatic decline in performance occurs when 30 wt.% MEA is used. Interfacial tension and contact angle measurements show that 20 wt.% MEA has a surface tension of 66.9 ± 0.6 mN/m and contact angle of $117 \pm 4^\circ$ with PP which is not dissimilar to that of 30 wt.% MEA (66.0 ± 0.4 mN/m and $116 \pm 2^\circ$). However, since the viscosity of 30 wt.% MEA (1.9 mPa/s (14)) is substantially higher than that of 20 wt.% MEA

Table 2. Change in performance of PP membrane cartridge over time using 20 wt.% MEA solution for liquid flow rate of 2.42 m^3/m^2hr and liquid flow through contactor shell

Hours of absorption previous to data collection	$K_G a_v$ (kmol/m^3kPa · hr)
0	4.81
165	2.80
% Reduction in mass transfer rate	42

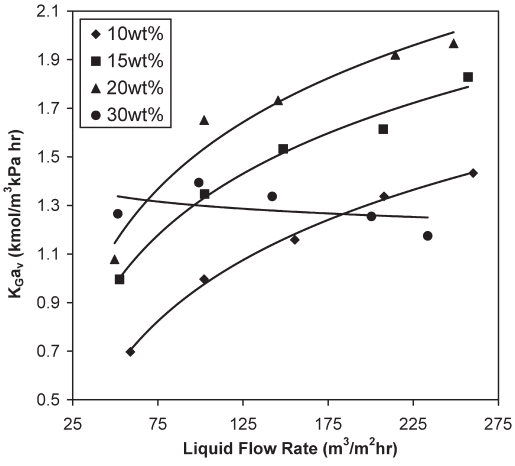

Figure 4. Relationship between overall mass transfer coefficient and MEA concentration for PP membrane cartridge. Liquid flow through fiber lumen. The solid lines highlight the general trends for each data set.

(1.4 mPa/s) the corresponding pressure drop across the length of the hollow fibers will increase (Table 3). Assuming a constant gas side pressure, this will lead to an increase in the transmembrane pressure difference and will likely cause membrane-liquid breakthrough (see Equation (1)) and hence pore wetting. A transmembrane pressure difference of up to 50 kPa was used for each experiment and based on Equation (1), the theoretical breakthrough pressure of 30 wt.% MEA through PP membrane is expected to be 46 kPa (compared to a breakthrough pressure of 49 kPa for 20 wt.% MEA).

This pore wetting means that the membrane resistance ($1/k_m$) will increase dramatically and hence the overall mass transfer coefficient decreases. Further, as the liquid boundary layer contributes proportionately less to mass transfer, there is no upward trend in this coefficient with liquid flow rate despite the higher liquid Reynolds number for higher liquid velocities (Table 3).

In addition, further experiments with 10 and 20 wt.% MEA following drying of the same PP fibers yielded K_Ga_v values of less than 0.3 kmol/m^3kPa · hr which shows that fiber wetting and degradation is permanent and irreversible.

A well-established method based on a heat transfer analogy proposed by Wilson (15) can be used to determine the magnitude of the individual resistances as well as the dependence of the overall resistance on the liquid velocity. It is valid in situations operating under steady-state where the only variable is the fluid velocity. It is a two-step calculation which consists of calculating the overall mass transfer coefficient for each experiment and plotting the overall mass transfer resistance as a function of the inverse liquid Reynolds number (see Equation (5)). Since the gas and membrane resistances are not a

Table 3. Dependence of liquid Reynolds number (Re_l) and pressure drop across the hollow fiber length on aqueous MEA concentration and velocity. Values for the lowest and highest liquid flow rates through the fiber lumen of the 275 fiber PP membrane cartridge are shown

Concentration (wt.%)	Velocity, U_l (m/s)	Flow rate (mL/min)	Re_l (−)	Pressure drop (kPa)[a]
20	0.014	17	3.09	0.90
30	0.014	17	2.28	1.23
20	0.072	83	15.43	4.52
30	0.072	83	11.39	6.13

Length of membrane contactor *L*: 12.7 cm; Inside diameter of hollow fiber: 0.300 mm. Viscosity of solution μ_{MEA}: 1.4×10^{-3} kg/ms (20 wt.%), 1.9×10^{-3} kg/ms (30 wt.%). Density of solution ρ_{MEA}: 1008 kg/m^3 (20 wt.%), 1010 kg/m^3 (30 wt.%).

[a]Pressure drop predicted using Hagen-Poiseuille Law.

function of the liquid velocity, the addition of these resistances corresponds to the intercept of this plot.

$$\frac{1}{K_G} = \underbrace{\text{slope} \times \frac{1}{\text{Re}^z}}_{\text{function of } \frac{1}{k_l}} + \underbrace{\text{intercept}}_{\frac{1}{k_g}+\frac{1}{k_m}} \tag{5}$$

Figure 5 is the Wilson plot for PVDF, PTFE and both previously unused PP and PP that has been exposed to MEA. An exponent (z) of 0.9 was chosen to achieve the best fit for the lines according to the least squares method and is comparable to exponents used in the literature which range from 0.6–0.9 (9, 16, 17).

An empirical correlation has been used to estimate the gas resistance and thereby determine the resistance imposed by the membrane from the intercept of the Wilson plot. Although a number of correlations have been proposed, the gas shell-side mass transfer coefficient is not well understood (18). Much of this uncertainty arises because it is a function of the fluid hydrodynamics of the shell-side which is dependent on the packing density and uniformity of the fiber spacing. The following correlation was developed for gas shell-side flow parallel to hollow fibers for gas absorption and stripping (16).

$$Sh = 1.25\left(\text{Re}\frac{d_e}{L}\right)^{0.93} Sc^{1/3} \tag{6}$$

Equation (6) is valid for $0.5 < \text{Re} < 500$, was tested for module packing fractions of 0.3 and 0.26 and has been used to evaluate the gas resistance in this work. However, other correlations give similar predictions (19, 20).

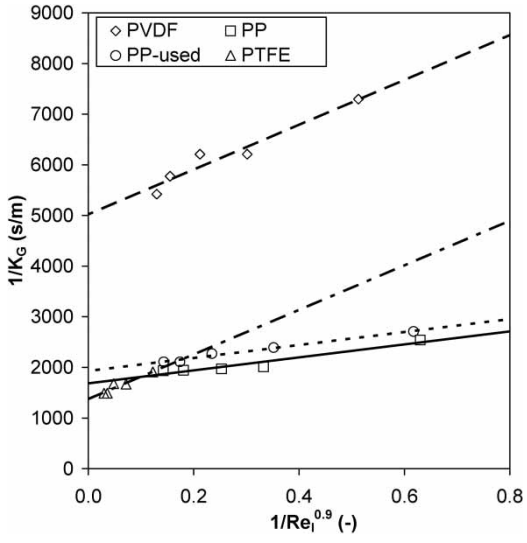

Figure 5. Wilson plot for PVDF (– – –), PP (previously unused) (—), PP-used (used in CO_2 absorption experiments for 45 hours) (– – –) and PTFE (-·-·-) membrane cartridges. All experiments were performed with 20 wt.% MEA flowing through the fiber lumen.

Table 4 shows the contribution of each resistance to the total resistance when evaluated at a Reynolds number in the liquid phase of approximately 2.2. As expected, the gas resistance is low, while the liquid or the membrane resistances are dominant. In particular, the membrane contributes a significant proportion of the overall resistance to mass transfer. Owing to their larger external fiber diameter and therefore larger equivalent shell-side diameter, the gas resistance is lower for the PVDF and PTFE membrane cartridges. However, the gas resistance contributes less than 11% of the overall resistance in all cases.

The PVDF cartridge performs at the lowest level for all liquid flow rates (Fig. 5). This conclusion conflicts with the results of Yeon et al. (10) and Matsumoto et al. (11). However, as pointed out earlier, these authors compared membrane materials with widely different pore sizes. Their conclusions can thus be related more to pore size than to any underlying properties of the membrane materials.

The PTFE cartridge performs better than the fresh PP for $Re_l \geq 13$ and better than the partially degraded PP for $Re_l \geq 7$. The membrane resistance of the PTFE membrane is 7% lower than that of the fresh PP and 21% lower than that of the partially degraded PP cartridge. The drop in performance of the PP membrane with increasing absorption time can be attributed to an increase in the membrane resistance. After 45 hours of operation, the membrane resistance increases by approximately 15%.

Table 4. Estimated resistances for PVDF, PP (previously unused), PP-used (used in CO_2 absorption experiments for 45 hours) and PTFE membrane cartridges calculated using the Wilson-plot method

	Resistances (s/m)					Contribution to overall resistance (%)		
Membrane	Overall ($Re_l = 2$)	Membrane + gas (intercept)	Slope	Gas[a]	Membrane	Liquid overall	Gas overall	Membrane overall
PTFE	3575	1375	4399	53	1322	61.5	1.5	37.0
PP	2326	1685	1282	257	1429	27.6	11.0	61.4
PP-used	2570	1930	1281	257	1673	24.9	10.0	65.1
PVDF	7233	5021	4423	137	4884	61.2	1.9	67.5

[a]Gas resistance evaluated using an empirical correlation (Equation (6)).

Membrane Characterization

Membrane-solvent wettability can be experimentally measured using the contact angle. The surface tension of a liquid mixture which has a contact angle of 90° on a membrane surface (γ_L^{90}) corresponds to the minimum surface tension liquid that can be used before the surface will become wetted. It can be used to approximate the maximum concentration of MEA in water that can be used without the membrane surface becoming wetted (although allowance must be made for surface degradation due to prolonged exposure to MEA). The critical surface tension of wetting (γ_c) is the surface tension of a liquid mixture which has a contact angle of 0° on a membrane surface. This value gives important information regarding the surface energy of the polymer material.

However, contact angles can only provide information about the wettability of the surface under atmospheric pressure conditions. A theoretical breakthrough pressure (P_{BP}) can also be calculated from Equation (1) that can be used to predict the wettability of the membrane under more realistic processing conditions because it simulates the pressurised liquid-vapour interface that is formed at the pore entrance of the membrane during the absorption process. Table 5 displays wettability data for the three membrane materials.

PTFE material has the highest hydrophobicity (or lowest surface energy) followed by PVDF and PP (21, 22). However, both the breakthrough pressure and contact angles with water and MEA on PVDF are lower than on PP. This anomaly was also found by Franken et al. (21) and Keurentjes et al. (23) on PVDF membrane surfaces and is likely to be a property of the membrane surface, possible arising due to the membrane casting procedure used for PVDF. The breakthrough pressure and contact angles for PTFE are highest, followed by PP and PVDF which is in agreement with the CO_2 absorption rates found and suggest that PVDF and PP have lower absorption rates than PTFE primarily due to membrane wetting and a correspondingly higher membrane resistance. PTFE also retains its hydrophobicity on contact with MEA, while the PP and PVDF membranes undergo degradation shown by a drop in water contact angle by up to 24° on PP and 22° on PVDF after MEA contact.

The decrease in performance of the PP membrane over time can be explained by examining SEM images of fresh PP fibers and fibers that have been used in absorption experiments with liquid flow in both the fiber lumen and contactor shell (Fig. 6). Profiles of the inside and outside of PP show that after extended contact with MEA, the membrane surface changes in morphology by becoming less textured. It also appears to have lost some porosity. This behavior was also observed by Wang et al. (24) and Barbe et al. (25) who found an increase in the average pore diameter and a change in the shape of the pores due to amine solvent exposure.

Chemical changes also occur to reduce the performance of PP during the absorption process. XPS analysis of the inside surface of both unused PP

Table 5. Membrane material wettabilities. Data measured/compiled for model flat membrane surfaces

Polymer type	PP	PTFE	PVDF
Manufacturer	Membrana Accurel (Germany)	Sartorius (Germany)	Millipore (Australia)
Price (USD/m^2)	51	2775	786
Average pore size (μm)	0.1	0.2	0.1
Water contact angle	127 ± 2	140 ± 5	117 ± 9
20 wt.% MEA contact angle	117 ± 4	127 ± 2	97 ± 8
Water contact angle after MEA exposure	110 ± 5	138 ± 3	107 ± 3
Breakthrough pressure (kPa)	$24 - 30$	$66 - 70$	0
Surface tension of liquid mixture which has a contact angle of 90° on a membrane surface (γ_L^{90}) [mN/m] (21)	55[a]	40.5[a]	50[a]
Critical surface tension of wetting (γ_c) [mN/m] (21, 22)	29[a]	18[a]	25[a]

[a]Values sourced from literature.

hollow fiber and PP that has been exposed to a CO_2/air stream show an increase in the elemental oxygen on the surface from 0.78 to 1.49% (Table 6). This could be due to oxidation of the PP membrane. The membrane was in direct contact with a CO_2/air stream for 68 hours and the thermal oxidation of PP is documented to occur at slow rates in air at atmospheric pressure and relatively low temperatures (26). Another possible cause for an increase in oxygen on the surface is chemical reactions between the membrane and MEA. This was also suggested by Wang et al. for the contact of PP membrane with DEA solution (24). Incorporation of additional oxygen into the PP surface will reduce its hydrophobicity and increase the likelihood of pore wetting in the presence of MEA and other low surface tension solvents.

CONCLUSIONS AND RECOMMENDATIONS

With respect to their CO_2 absorption performance in MEA, the membrane materials can be ranked in the order PTFE > PP > PVDF. However, none of the materials will be ideal for use with MEA. Both wettability analyses and CO_2 absorption tests have shown that PVDF is unsuitable for use with MEA. While PP performs well initially, its performance drops over longer periods of time and with the use of more concentrated MEA solutions. This drop in performance seems to have no lower limit and corresponds to an increase in the membrane resistance by 15% after 165 hours which is most

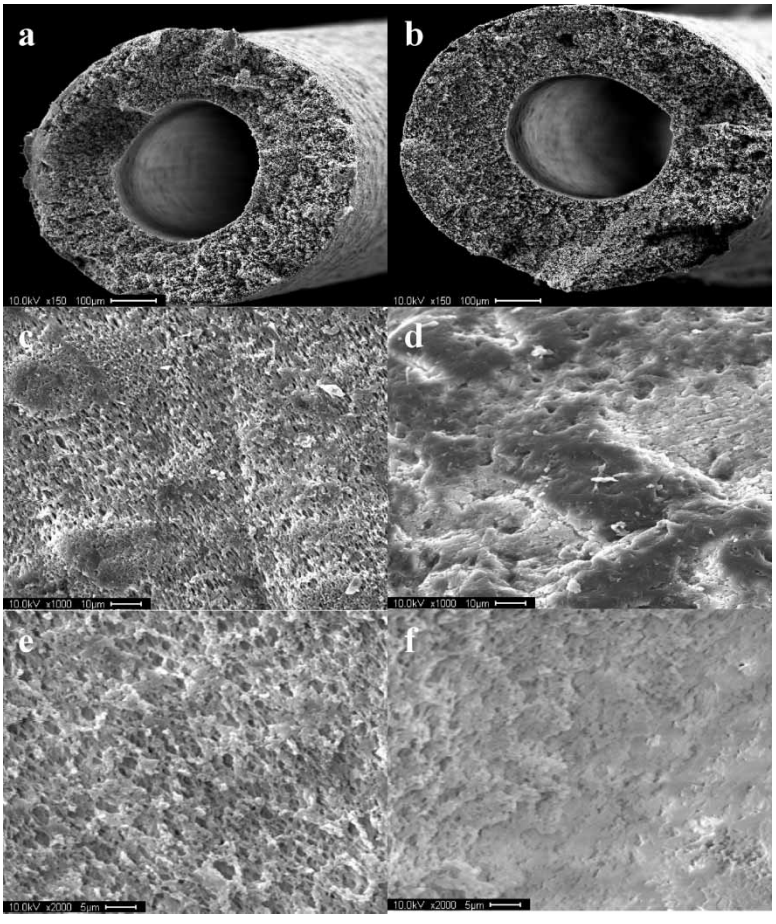

Figure 6. SEM of PP hollow fiber. a/b: top profile of unused/used hollow fiber (150× magnification); c/d: side profile of outside of unused/used hollow fiber (1000× magnification); e/f: side profile of inside of unused/used hollow fiber (2000× magnification).

Table 6. Mass concentrations (%) found by XPS measurements of the inside surfaces of unused and used PP membranes

Atom	PP	PP-used[a]
O	0.78	1.49
C	99.22	98.51

[a]PP-used has been subject to CO_2 absorption experiments with 20 wt.% MEA solution for 68 hours.

likely due to membrane degradation (and consequently wetting) by the solvent. PTFE is extremely hydrophobic and inert and it performs well. However, it is expensive and it is not as readily available with small pore sizes as the alternatives.

Future research should focus on either the development of new solvents or membrane materials. New solvents should have similar properties to MEA but higher surface tensions. This would allow the use of cheap membrane materials such as PP and is being investigated by some research groups (27). The alternative is the development of more resilient and higher performing membrane materials that can be used with MEA. Cheap surface treatments that increase the durability of PP to MEA and allow it to sustain its performance over time may result in significant cost improvements for the process.

APPENDIX A

The overall mass transfer coefficient (K_G) which is based on pressure was calculated using a similar method used for absorption in a packed column system. The CO_2 molar flux (N) is given by the product of the gas phase mass transfer coefficient based on pressure (k_g) and the CO_2 partial pressure driving force in the gas phase:

$$N = k_g\left(P_{CO_2} - P^*_{CO_2}\right) \tag{7}$$

where P_{CO_2} is the CO_2 partial pressure and $P^*_{CO_2}$ is the equilibrium CO_2 partial pressure at the gas-liquid interface. For an element of length (dL) the change in concentration of the gas phase is equal to the change in concentration in the liquid phase which leads to the expression:

$$G \cdot dY = k_g \cdot a_v\left(P_{CO_2} - P^*_{CO_2}\right)a \cdot dL \tag{8}$$

where a is the cross-sectional area of the membrane contactor, a_v is the area per unit volume, G is the inert gas flow rate and Y is the CO_2 mole ratio which is given by:

$$Y = \frac{\text{moles of solute}}{\text{moles of inert gas}} = \frac{y}{1-y} = \frac{P_{CO_2}}{P - P_{CO_2}} \tag{9}$$

where y is the CO_2 mole fraction in the gas phase and P is the total pressure. Rearranging the expression for the mass transfer coefficient and substituting $P_{CO_2} = yP$ gives the formula used to calculate the product of the overall mass transfer coefficient and area per unit volume:

$$K_G a_v = \frac{G}{aP(y - y^*)}\frac{dY}{dL} \tag{10}$$

For chemical absorption, the equilibrium mole fraction of CO_2 in the gas phase (y^*) is equal to zero. Note that while this calculation is ideal for use with packed columns, it should be used with care for hollow fiber modules where the cross-sectional area for flow of the gas phase may vary due to a different number of hollow fibers or fibers with different geometries being used. For a larger cross-sectional area, the inert gas flow rate per unit cross-section of the membrane contactor (G/a) will be correspondingly smaller which will lead to a smaller mass transfer coefficient despite the use of an identical inert gas flow rate (G).

NOMENCLATURE

A	Mass transfer area (m^2)
a	Cross-sectional area of membrane contactor (m^2)
a_v	Specific surface area (m^2/m^3)
D	CO_2 diffusivity (m^2/s)
d_e	Equivalent diameter (4 × cross-sectional area for flow/wetted perimeter) (m)
d_{max}	Maximum pore diameter of membrane (m)
E	Enhancement due to reaction (−)
G	Inert gas flow rate (mol/s)
k	Individual phase mass transfer coefficient (m/s)
K_G	Overall mass transfer coefficient ($kmol/m^2kPa \cdot hr$)
L	Length of hollow fiber contactor (m)
m	Partition coefficient (−)
N	CO_2 flux (mol/m^2s)
P_{CO_2}	CO_2 partial pressure (kPa)
P_{BP}	Breakthrough pressure (Pa)
P_T	Total pressure (kPa)
Re	Reynolds number, $\frac{\rho_g U_g d_e}{\mu_g}$ (−)
Sc	Schmidt number, $\frac{\mu_g}{\rho_g D_g}$ (−)
Sh	Sherwood number, $\frac{k_g d_e}{D_g}$ (−)
U	Fluid velocity (m/s)
x	Contactor height (m)
y	CO_2 mole fraction in gas (−)
Y	CO_2 mole ratio in gas (−)
ρ	Density (kg/m^3)
μ	Viscosity (kg/ms)
γ_c	Critical surface tension (has 0° contact angle on membrane surface) (mN/m)

γ_L^{90}	Surface tension of liquid with 90° contact angle on membrane surface (mN/m)
γ_{lg}	Surface tension of liquid (N/m)
θ	Contact angle of liquid on membrane (°)

Superscripts

*	In equilibrium
z	Exponent in Equation (5)

Subscripts

g	Gas
m	Membrane
l	Liquid
MEA	Property relating to MEA solvent
in	Entering membrane contactor
out	Exiting membrane contactor

ACKNOWLEDGMENTS

The authors would like to thank the Cooperative Research Centre for Greenhouse Gas Technologies (CO2CRC), Particulate Fluids Processing Centre (PFPC) and Australian Research Council (ARC) for financial assistance. Also, the receipt of a Melbourne University Postgraduate Overseas Research Scholarship (PORES) and help from Harald Berwald and the workshop at the University of Regina allowed absorption experiments to be conducted at the International Test Centre for CO_2 Capture, Canada. The authors would also like to acknowledge Paul Pigram and Penelope Hale for assistance provided with XPS analysis and Kang Li and the University of Bath for donation of the PVDF fibers.

REFERENCES

1. Metz, B., Davidson, O., de Coninck, H., Loos, M., and Meyer, L. (2005) *Carbon Dioxide Capture and Storage: Summary for Policymakers,* in *IPCC Special Report*; Intergovernmental Panel on Climate Change: Geneva.
2. Steeneveldt, R., Berger, B., and Torp, T.A. (2006) CO_2 capture and storage: closing the knowing doing gap. *Chem. Eng. Res. Des.*, 84 (A9 Carbon Capture and Storage): 739.

3. Falk-Pedersen, O., Gronvold, M.S., Nokleby, P., Bjerve, F., and Svendsen, H.F. (2005) CO_2 capture with membrane contactors. *International Journal of Green Energy*, 2 (2): 157.
4. Kohl, A. and Nielsen, R. (1997) *Gas Purification*, 5th edn.; Gulf Publishing Company: Houston, 41.
5. Rangwala, H. (1996) Absorption of carbon dioxide into aqueous solutions using hollow fiber membrane contactors. *J. Membr. Sci.*, 112 (2): 229.
6. deMontigny, D., Tontiwachwuthikul, P., and Chakma, A. (2006) Using polypropylene and polytetrafluoroethylene membranes in a membrane contactor for CO_2 absorption. *J. Membr. Sci.*, 277 (1–2): 99.
7. Nishikawa, N., Ishibashi, M., Ohta, H., Akutsu, N., Matsumoto, H., Kamata, T., and Kitamura, H. (1995) CO_2 removal by hollow-fiber gas-liquid contactor. *Energy Conversion and Management*, 36 (6–9): 415.
8. Wang, D., Li, K., and Teo, W.K. (1999) Preparation and characterization of polyvinylidene fluoride (PVDF) hollow fiber membranes, 163 (2): 211.
9. Atchariyawuta, S., Feng, C., Wang, R., Jiraratananona, R., and Liang, D.T. (2006) Effect of membrane structure on mass-transfer in the membrane gas-liquid contacting process using microporous PVDF hollow fibers. *J. Membr. Sci.*, 285 (1–2): 272.
10. Yeon, S.-H., Sea, B., Park, Y.-I., and Lee, K.-H. (2003) Determination of mass transfer rates in PVDF and PTFE hollow fiber membranes for CO_2 absorption. *Sep. Sci. Technol.*, 38 (2): 271.
11. Matsumoto, H., Kitamura, H., Kamata, T., Ishibashji, M., and Ota, H. (1995) Effect of membrane properties of microporous hollow-fiber gas-liquid contactor on CO_2 removal from thermal power plant flue gas. *Journal of Chemical Engineering of Japan*, 28 (1): 125.
12. Horowitz, W. (1974) *Official Methods of Analysis of the Association of Official Analytical Chemists*, 12th edn.; Washington Association of Official Analytical Chemists: Washington, DC.
13. deMontigny, D., Tontiwachwuthikul, P., and Chakma, A. (2001) Parametric studies of carbon dioxide absorption into highly concentrated monoethanolamine solutions. Can. *J. Chem. Eng.*, 79 (1): 137.
14. Lee, M.-J. and Lin, T.-K. (1995) Density and viscosity for monoethanolamine + water, + ethanol, and + 2-propanol. *J. Chem. Eng. Data*, 40 (1): 336.
15. Wilson, E.E. (1915) A basis for rational design of heat transfer apparatus. *Trans. ASME*, 37: 47.
16. Yang, M.C. and Cussler, E.L. (1986) Designing hollow-fiber contactors. *AIChE J.*, 32 (11): 1910.
17. Viegas, R.M.C., Rodríguez, M., Luque, S., Alvarez, J.R., Coelhoso, I.M., and Crespo, J.P.S.G. (1998) Mass transfer correlations in membrane extraction: Analysis of Wilson-plot methodology. *J. Membr. Sci.*, 145 (1): 129.
18. Gabelman, A. and Hwang, S. (1999) Hollow fiber membrane contactors. *J. Membr. Sci.*, 159: 61.
19. Prasad, R. and Sirkar, K. (1998) Dispersion-free solvent extraction with microporous hollow-fiber modules. *AIChE J.*, 34 (2): 177.
20. Dahuron, L. and Cussler, E. (1988) Protein extractions with hollow fibers. *AIChE J.*, 34 (1): 130.
21. Franken, A.C.M., Nolten, J.A.M., Mulder, M.H.V., Bargeman, D., and Smolders, C.A. (1987) Wetting criteria for the applicability of membrane distillation. *J. Membr. Sci.*, 33 (3): 315.

22. Johnson, R.E., Jr. and Dettre, R.H. (1964) Contact angle hysteresis. III. Study of an idealized heterogeneous surface. *Journal of Physical Chemistry*, 68 (7): 1744.
23. Keurentjes, J.T.F., Harbrecht, J.G., Brinkman, D., Hanemaaijer, J.H., Stuart, M.A.C., and Van't Riet, K. (1989) Hydrophobicity measurements of microfiltration and ultrafiltration membranes. *J. Membr. Sci.*, 47 (3): 333.
24. Wang, R., Li, D.F., Zhou, C., and Liang, D.T. (2004) Impact of DEA solutions with and without CO_2 loading on porous polypropylene membranes intended for use as contactors. *J. Membr. Sci.*, 229 (1–2): 147.
25. Barbe, A.M., Hogan, P.A., and Johnson, R.A. (2000) Surface morphology changes during initial usage of hydrophobic, microporous polypropylene membranes. *J. Membr. Sci.*, 172 (1–2): 149.
26. Rychly, J., Matisova-Rychla, L., Csmorova, K., Achimsky, L., Audouin, L., Tcharkhtchi, A., and Verdu, J. (1997) Polymer degradation and stability. *Polym. Degrad. Stab.*, 58 (3): 269.
27. Feron, P. and Jansen, A. (2002) CO_2 Separation with polyolefin membrane contactors and dedicated absorption liquids: performances and prospects. *Sep. Purif. Technol.*, 27: 231.